Probing the top-Higgs boson FCNC couplings via the $h \to \gamma\gamma$ channel at the HE-LHC and FCC-hh

Yao-Bei Liu[1,*] and Stefano Moretti[2,†]

[1]*Henan Institute of Science and Technology, Xinxiang 453003, People's Republic of China*
[2]*School of Physics and Astronomy, University of Southampton, Highfield, Southampton SO17 1BJ, United Kingdom*

(Received 11 February 2020; accepted 4 April 2020; published 15 April 2020)

We investigate the sensitivity of future searches for the top-Higgs boson flavor changing neutral current (FCNC) couplings tqh ($q = u$, c) at the proposed High Energy Large Hadron Collider (HE-LHC) and Future Circular Collider in the hadron-hadron mode (FCC-hh). We perform a full simulation for the two processes in the $h \to \gamma\gamma$ decay channel (where h is the discovered Higgs boson state): the single top quark FCNC production in association with the Higgs boson (plus a jet) and the top quark pair production with FCNC decays $t \to qh$. All the relevant backgrounds are considered in a cut based analysis to obtain the limits on the branching ratios (BRs) of $t \to uh$ and $t \to ch$. It is shown that, at the HE-LHC with an integrated luminosity of 15 ab^{-1} and at the FCC-hh with an integrated luminosity of 30 ab^{-1}, the BR$(t \to uh)$ [BR$(t \to ch)$] can be probed, respectively, to $7.0(8.5) \times 10^{-5}$ and $2.3(3.0) \times 10^{-5}$ at the 95% confidence level (C.L.) (assuming a 10% systematic uncertainty on the background), which is almost 2 orders of magnitude better than the current 13 TeV LHC experimental results.

DOI: 10.1103/PhysRevD.101.075029

I. INTRODUCTION

The discovery of a 125 GeV Higgs boson [1,2] at the Large Hadron Collider (LHC)[1] was a landmark in the history of particle physics, and it has opened up a new area of direct searches for beyond the standard model (BSM) phenomena, since the h state may well be the portal into a new physics (NP) world. Possible signals of NP are flavor changing neutral current (FCNC) interactions between the Higgs boson, the t quark, and a u or c quark, i.e., the vertex tqh ($q = u$, c). In the SM, the FCNC top quark decays $t \to qh$ ($q = u$, c) are forbidden at the tree level and strongly suppressed at the loop level due to the Glashow-Iliopoulos-Maiani (GIM) mechanism [3]. For instance, the predicted BR$(t \to qh)$'s with $q = u$, c are expected to be of $\mathcal{O}(10^{-12}$–$10^{-17})$ [4–6] at the one-loop level and are therefore out of range for current and near future experimental sensitivity. However, in some NP models the BRs for the $t \to qh$ decays are predicted to be in the range of $\mathcal{O}(10^{-6}$–$10^{-3})$ [7–19]. Thus, any observation of such FCNC processes would be a clear signal of BSM dynamics.

Recently, the most stringent constraint on the top-Higgs boson FCNC couplings through direct measurements was reported by the CMS and ATLAS Collaborations [20–25], by searching for $t\bar{t}$ production with one top decaying to Wb and the other assumed to decay to hq. Corresponding to 36.1 (35.9) fb^{-1} of data at the center-of-mass (c.m.) energy of 13 TeV for ATLAS (CMS), the 95% confidence level (C.L.) upper limits are summarized in Table I. In addition to the direct collider measurements, indirect constrains on an anomalous tqh vertex can be obtained from the observed $D^0 - \bar{D}^0$ mixing and $Z \to c\bar{c}$ decays, where the upper limits of BR$(t \to qh) < 5 \times 10^{-3}$ [26] and BR$(t \to qh) < 0.21\%$ [27] are obtained, respectively. From a phenomenological viewpoint, the top-Higgs boson FCNC interactions have

TABLE I. The current experimental upper limits on top-Higgs boson FCNC decays at 95% C.L.

Detector	Decay channel	BR$(t \to uh)$	BR$(t \to ch)$
ATLAS, 13 TeV, 36.1 fb^{-1}	$h \to \gamma\gamma$ [22]	2.4×10^{-3}	2.2×10^{-3}
	Multilepton states [23]	1.9×10^{-3}	1.6×10^{-3}
	$h \to b\bar{b}$ [24]	5.2×10^{-3}	4.2×10^{-3}
	$h \to \tau^+\tau^-$ [24]	1.7×10^{-3}	1.9×10^{-3}
CMS, 13 Tev, 35.9 fb^{-1}	$h \to b\bar{b}$ [25]	4.7×10^{-3}	4.7×10^{-3}

*liuyaobei@hist.edu.cn
†Es.moretti@soton.ac.uk
[1]Henceforth, it will be denoted by the symbol h.

been studied extensively at hadron colliders within many NP scenarios [28–38]. Besides, many phenomenological studies using model-independent methods have also been performed via either anomalous top decay or anomalous top production processes [39–44].

A more promising result was put forward by the ATLAS Collaboration [45,46], which has predicted the sensitivities $\mathrm{BR}(t \to uh) < 2.4 \times 10^{-4}$ and $\mathrm{BR}(t \to ch) < 1.5 \times 10^{-4}$ at 95% C.L. at the High Luminosity LHC (HL-LHC). One can expect to improve further these limits at higher c.m. energies [47]. The future High Energy LHC (HE-LHC) with 27 TeV c.m. energy [48] and the Future Circular Collider in hadron-hadron mode (FCC-hh) with 100 TeV c.m. energy [49] have great potential to pursue direct evidence of top-Higgs boson FCNC couplings with integrated luminosities of 15 ab^{-1} and 30 ab^{-1} in their final stages, respectively. While rather distant in the future, there are a lot of studies in literature that have shown how these machines can greatly improve the scope of previous accelerators in pursuing BSM searches [50–53]. So it is rather appropriate to assess their scope in accessing tqh vertices too, the main reason being the common prejudice in the particle physics community that BSM phenomena are likely to manifest themselves in the interactions between the two heaviest states of the SM, indeed t and h, which are in fact intimately related to the hierarchy problem of the SM, the main puzzle that nature has forced upon us.

In our present paper, we perform an updated study of top-Higgs boson FCNC interactions at the HE-LHC and FCC-hh, by considering both single top quark production in association with the Higgs boson (plus a jet) and top quark pair production followed by a Higgs decay of one (anti)top state. A previous study done in Ref. [54] has investigated the top-Higgs boson FCNC interactions through $pp \to thj$ with the subsequent decays $t \to b\ell^+\nu$ and $h \to \gamma\gamma$ at the HL-LHC. Here, we intend to revisit that analysis in the context of the aforementioned higher energy and luminosity hadron machines.

Furthermore, past literature also included the study of a single top and Higgs boson associated production via the process $pp \to th$, affording one with an improved sensitivity to especially the tuh coupling (and somewhat less so to the tch one) [25]. Specifically, the authors of Ref. [55] investigated the top-Higgs boson FCNC interactions through the $pp \to t(\to b\ell^+\nu)h(\to\gamma\gamma)$ process at the HL-LHC. However, one realizes that the final numbers of events for these signals at the 14 TeV LHC are too small against the overwhelming SM background rate, even considering the high luminosity option of 3 ab^{-1}, and also because the signals suffer from a small BR (0.23%) for the $h \to \gamma\gamma$ channel. Yet, this is possibly the cleanest probe of the SM-like Higgs boson, so it ought to be nonetheless explored. In contrast, at both the HE-LHC and FCC-hh, the same production cross sections for signal (and SM background) can be enhanced significantly due to the higher energies available therein, so that one can find it a more favorable environment than the 13 and 14 TeV LHC to study the top-Higgs boson FCNC couplings via the $h \to \gamma\gamma$ decay channel, at the same time benefiting a larger luminosity.

In short, here, by studying the $pp \to thj$ process (i.e., with an explicit light jet in the final state[2]) inclusively, we aim at treating on the same footing both single and double top production. This paper is arranged as follows. In Sec. II, we give a brief introduction to the top-Higgs boson FCNC couplings and perform a complete calculation of $pp \to thj$ by considering such interactions at tree level. In Sec. III, we discuss the observability (against the SM background) of such top-Higgs boson FCNC couplings through the process $pp \to thj$ with the top producing leptonic decay modes accompanied by $h \to \gamma\gamma$ at the HE-LHC and FCC-hh. Finally, conclusions and outlook are presented in Sec. IV.

II. TOP-HIGGS FCNC INTERACTIONS AND PRODUCTION PROCESSES

A. Top-Higgs boson FCNC couplings

Although the anomalous FCNC couplings between the top quark and Higgs boson may arise from different sources, an effective field theory approach can describe the effects of NP beyond the SM in a model-independent way [5]. The most general Lagrangian for the top-Higgs boson FCNC interactions is written as

$$\mathcal{L} = \kappa_{tuH}\bar{t}Hu + \kappa_{tcH}\bar{t}Hc + \mathrm{H.c.}, \tag{1}$$

where κ_{tuH} and κ_{tcH} represent the strength of top-Higgs boson FCNC interactions. In this study, we take them as real and symmetric, i.e., $\kappa_{tqH} = \kappa^\dagger_{tqH} = \kappa_{qtH} = \kappa^\dagger_{qtH}$ $(q = u, c)$, since we here do not intend to consider CP-violating effects.

The decay width of the dominant top quark decay mode $t \to Wb$ could be found in Ref. [56]. Neglecting the light quark masses and assuming the dominant top decay width $t \to Wb$, the next-to-leading order (NLO) $\mathrm{BR}(t \to qh)$ is given by [57,58]

$$\begin{aligned}\mathrm{BR}(t \to qh) &= \frac{\kappa^2_{tqH}}{\sqrt{2}m_t^2 G_F}\frac{(1-x_h^2)^2}{(1-x_W^2)^2(1+2x_W^2)}\lambda_{\mathrm{QCD}} \\ &\simeq 0.58\kappa^2_{tqh},\end{aligned} \tag{2}$$

with the Fermi constant G_F and $x_i = m_i/m_t (i = W, h)$. Here, the factor λ_{QCD} is the NLO QCD correction to $\mathrm{BR}(t \to qh)$ and equals about 1.1 [59–61]. In our work, we require $\kappa_{tqh} \leq 0.04$ to satisfy the direct constraint from the ATLAS result mentioned in the previous section.

[2]So that a direct comparison with existing experimental results can be made in the case of the $h \to b\bar{b}$ analysis of Ref. [24].

B. Production processes

At the LHC, the cross section for $pp \to thj$ involving top-Higgs boson FCNC couplings would be coming from two subprocesses: (i) top pair production followed by one FCNC top decay, $pp \to t\bar{t} \to thj$, shown in Figs. 1(a)–1(b) (henceforth referred to as "top FCNC decay"); (ii) single top-Higgs boson associated production in the presence of a jet, $pp \to thj$, as shown in Figs. 1(c)–1(f), which includes a gg (henceforth referred to as "tH associated production") and a qg (henceforth referred to as "qg fusion") induced subchannels, respectively, yielding a(n) (anti)quark or gluon in the final state. The contribution of other subprocesses, such as $q\bar{q}$ fusion channels, is smaller than the above ones due to the suppression from color factors and parton distribution functions (PDFs) and thus, is not shown in the Feynman diagrams, but all the contributions are included in our calculations. Obviously, the conjugated processes can also occur at tree level and are accounted for.

For the simulations of the HE-LHC and FCC-hh dynamics, we first use the FeynRules package [62] to extract the Feynman rules from the effective Lagrangian and to generate the universal FeynRules output (UFO) files and calculate the LO cross sections of $pp \to thj$ by using MadGraph5-aMC@NLO [63] with NNPDF23L01 PDFs [64], considering the renormalization and factorization scales to be $\mu_R = \mu_F = \mu_0/2 = (m_t + m_h)/2$. In our numerical calculations, the SM input parameters are taken as [65]

$$m_h = 125.1\,\text{GeV}, \quad m_t = 172.9\,\text{GeV}, \quad m_W = 80.379\,\text{GeV},$$
$$m_Z = 91.1876\,\text{GeV}, \quad \alpha_s(m_Z) = 0.1185,$$
$$G_F = 1.166370 \times 10^{-5}\,\text{GeV}^{-2}. \tag{3}$$

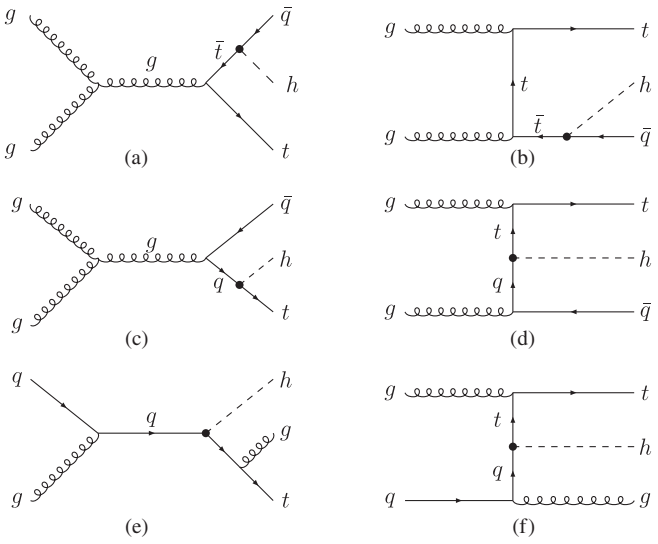

FIG. 1. Representative Feynman diagrams for: the gg fusion induced top pair production $gg \to t\bar{t}$ and $\bar{t} \to \bar{q}h$ decay (a)–(b), the gg fusion induced top-Higgs boson associated production $gg \to th\bar{q}$ (c)–(d), and the qg fusion induced top-Higgs boson associated production $qg \to thg$ (e)–(f). Here, $q = u, c$.

In Fig. 2, we show the dependence of the cross sections for the three thj subprocesses on the top-Higgs boson FCNC coupling parameter at the HE-LHC and FCC-hh for two scenarios, as follows: case I is for $\kappa_{tqh} = \kappa_{tuh}$, $\kappa_{tch} = 0$ whereas case II is for $\kappa_{tqh} = \kappa_{tch}$, $\kappa_{tuh} = 0$. The cuts on the transverse momentum (p_T^j) and pseudorapidity (η_j) of the extra jet are shown in the figures for both the HE-LHC and FCC-hh. From Fig. 2, one can see that, for a given coupling parameter κ_{tqh}, the production cross sections can be very significant at the higher c.m. energies of these two future machine. Besides, we also have the following observations.

(1) For both cases I and II, the dominant contribution to the thj final state is from (resonant) pair production, $pp \to t\bar{t} \to thj$. However, the other two contributions from tH associated production and qg fusion cannot be neglected, especially for case I. To be specific, in this scenario, when $\sqrt{s} = 27(100)$ TeV and $\kappa_{tuh} = 0.04$, the cross section of the top FCNC decay process is about 3.5 (30.9) pb while the cross section of the tH associated production process is about 1.7 (10.7) pb with the one for qg fusion being 1.3 (8.4) pb.

(2) For the same values of κ_{tuh} and κ_{tch}, the cross sections coming from the tH associated production and qg fusion processes in case I are much larger than those in case II: this is because the u quark has a larger PDF than that of the c quark. To be specific, in case II, when $\sqrt{s} = 27(100)$ TeV and $\kappa_{tch} = 0.04$, the cross section of the tH associated production process is only about 0.3 (3.1) pb while for qg fusion the rates are 0.19 (1.96).

III. DISCOVERY POTENTIAL

A. The signal-to-background analysis

In this section, we present the numerical calculations at the HE-LHC and FCC-hh of the processes,

$$pp \to t\bar{t} \to t(\to W^+b \to \ell^+\nu b)h(\to \gamma\gamma)j, \tag{4}$$

$$pp \to t(\to W^+b \to \ell^+\nu b)h(\to \gamma\gamma)j, \tag{5}$$

where $\ell = e, \mu$ and j represents [a(n) (anti)quark or gluon] jet, interfaced to the subsequent parton shower by using the MLM matching scheme [66,67]. The final state topology is thus characterized by two photons appearing as a narrow resonance centered around the SM-like Higgs boson mass, at least two jets with exactly one being tagged as b jet, one charged lepton and missing transverse momentum from the undetected neutrino. The main sources of background events that include both a Higgs boson decaying into diphotons in association with other particles and nonresonant production of $\gamma\gamma$ pairs are accounted for here:

(i) $pp \to t\bar{t}h$,
(ii) $pp \to thj$,

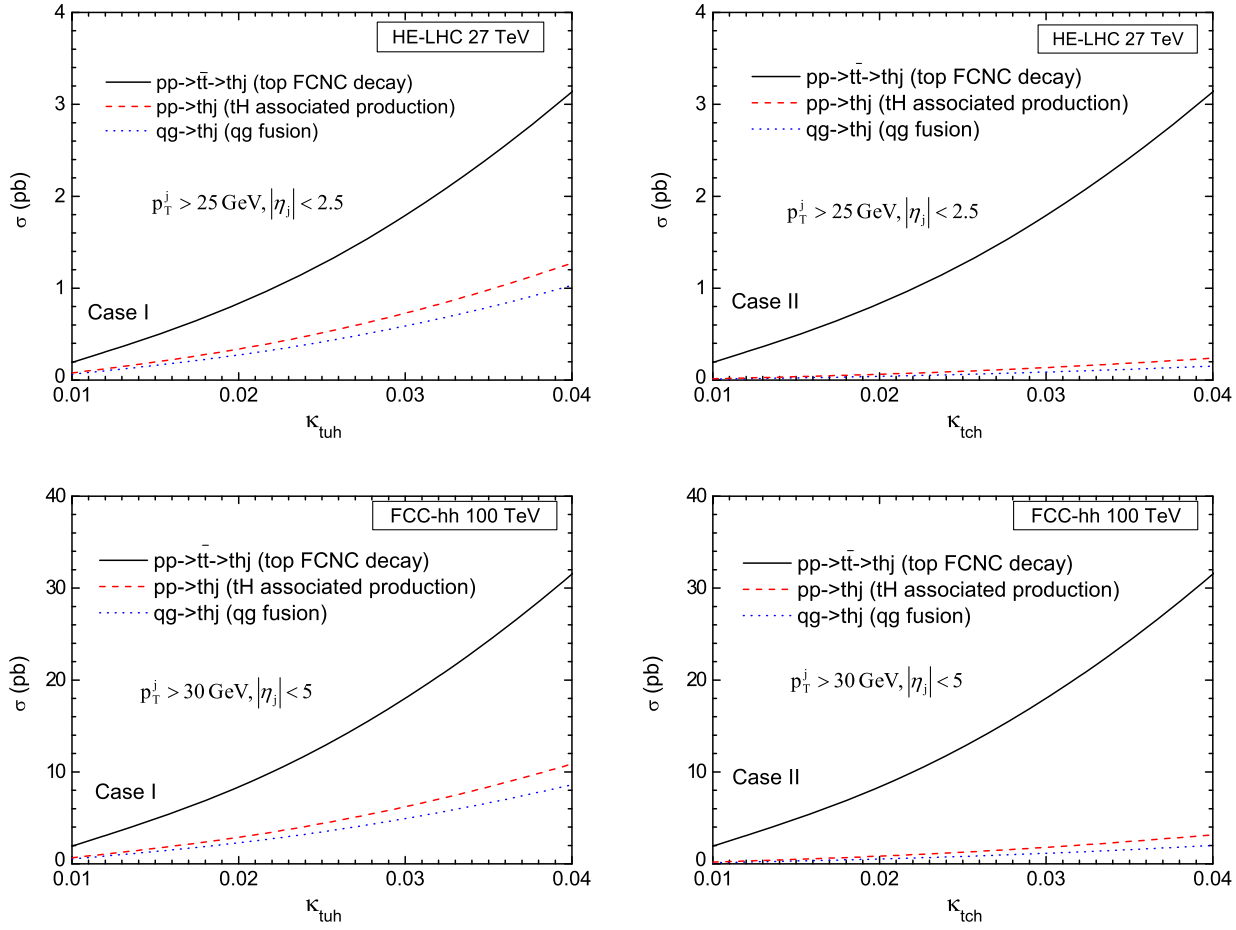

FIG. 2. The dependence of the cross section σ of the three $pp \to thj$ subprocesses of Fig. 1 on the top-Higgs boson FCNC couplings κ_{tqh} at the HE-LHC (top) and FCC-hh (bottom) for case I (left) and case II (right) identified in the text. Notice that the charge conjugated processes are also included in the calculation.

(iii) $pp \to W^{\pm}jjh$,
(iv) $pp \to t\bar{t}\gamma\gamma$,
(v) $pp \to tj\gamma\gamma$,
(vi) $pp \to \gamma\gamma W^{\pm}jj$.

The parton level events for the signal and the SM backgrounds are interfaced to a parton shower, fragmentation, and hadronization by using PYTHIA8.20 [68]. Then, we have passed all generated events through DELPHES3.4.2 [69] for detector simulation. Finally, event analysis is performed by using MadAnalysis5 [70]. As far as jet reconstruction is concerned, the anti-k_t algorithm [71] with a jet radius of 0.4 is used. For the HE-LHC and FCC-hh analysis, we have used the default HL-LHC and FCC-hh detector card configuration implemented into the aforementioned detector emulator.

The cross sections of the signal and dominant backgrounds at LO are adjusted to NLO QCD through K factors, i.e., $K = 1.4$ for the $pp \to t\bar{t} \to thj$ process [72], $K = 1.5$ for the tH associated production process [39,40], and $K = 1.3$ for the $pp \to t\bar{t}h$ process [72–74]. For the sake of simplicity, we have rescaled the other SM background processes by a K factor of 1.5. This approximation does not have a significant impact on our derived sensitivities and can be fully addressed in a future analysis.

In order to identify objects, we impose the following basic cuts to select the events [47]:

$$\begin{aligned}
&\mathrm{HE-LHC}: p_T^{\ell/j/b} > 25\,\mathrm{GeV}, \quad p_T^{\gamma} > 20\,\mathrm{GeV}, \\
&\qquad |\eta_i| < 2.5, \quad \Delta R_{ij} > 0.4 \quad (i,j = \ell, b, j, \gamma), \\
&\mathrm{FCC-hh}: p_T^{\ell/\gamma} > 25\,\mathrm{GeV}, \quad p_T^{j/b} > 30\,\mathrm{GeV}, \\
&\qquad |\eta_i| < 3, \quad \Delta R_{ij} > 0.4 \quad (i,j = \ell, b, j, \gamma), \qquad (6)
\end{aligned}$$

where ΔR is the angular distance between any two objects.

In order to choose appropriate kinematic cuts, in Fig. 3,[3] we plot some differential distributions for

[3]Hereafter, in figures and tables, by using "thj_tuh ($pp \to thj$ via tuh)" and "thj_tch ($pp \to thj$ via tch)", we will intend the contribution to the signal due to tH associated production plus qg fusion when only including the tuh or tch coupling on its own, respectively.

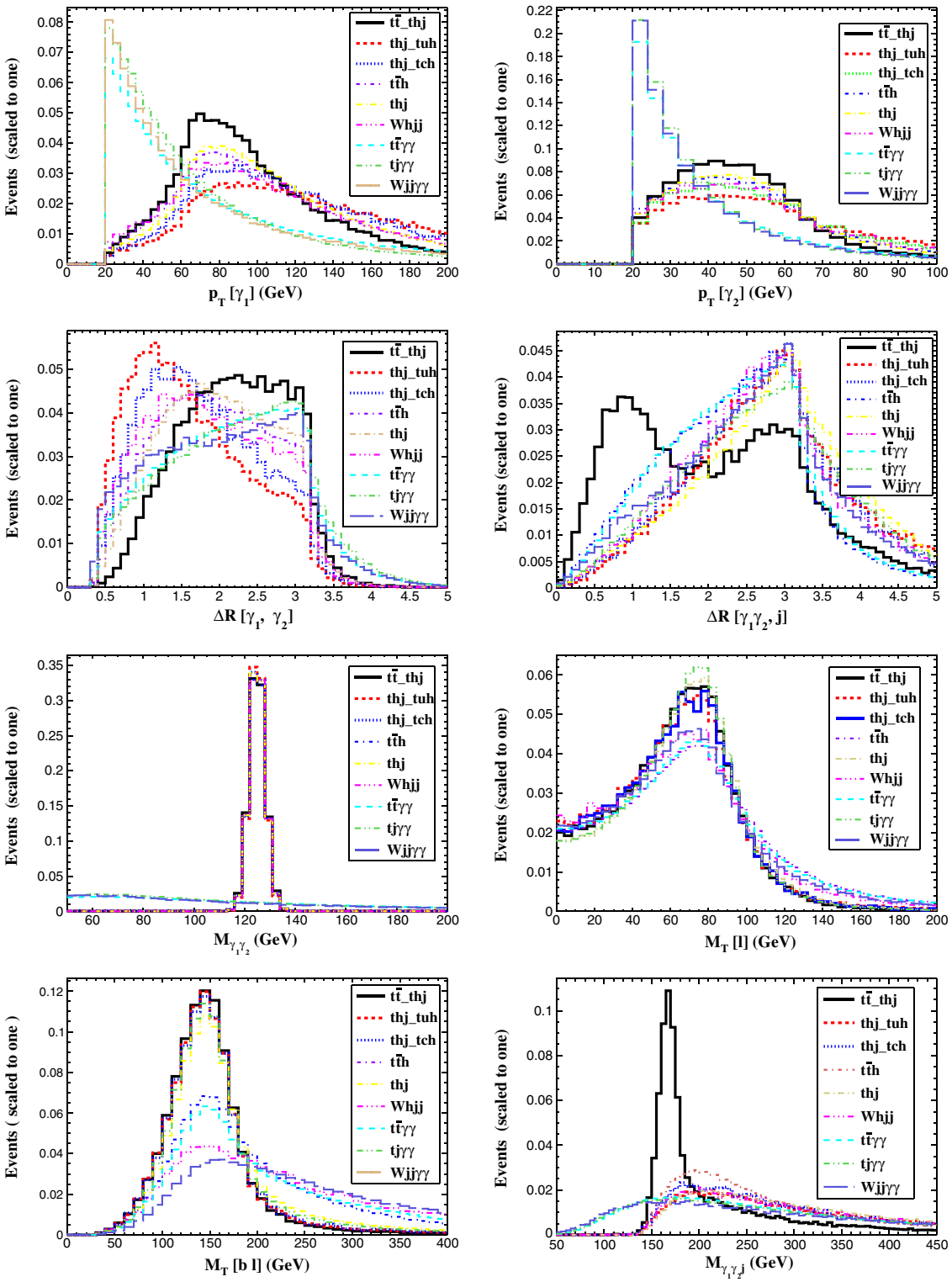

FIG. 3. Normalized distributions for the signals and SM backgrounds at LO for the HE-LHC at 27 TeV.

signals and SM backgrounds at the HE-LHC at 27 TeV, such as the (ordered) transverse momentum distributions of the two photons, $p_T^{\gamma_{1,2}}$, the separation, $\Delta R_{\gamma_1,\gamma_2}$ and $\Delta R_{\gamma_1\gamma_2,j}$, and invariant mass, $M_{\gamma\gamma}$, distributions of the two photons, the transverse mass distribution for the $\ell \not{E}_T$, $M_T(l)$, and $b\ell \not{E}_T$, $M_T(bl)$ systems, and the invariant mass, $M_{\gamma\gamma j}$. Based on these distributions, we impose a further set of cuts.

(i) Cut 1: Exactly one isolated lepton (electron or muon), at least two jets, and one of which must be b tagged.
(ii) Cut 2: At least two photons with $p_T^{\gamma_1} > 60$ GeV, $p_T^{\gamma_2} > 30$ GeV, since the two photons in the signal and resonant SM backgrounds come from the Higgs boson, they have a harder p_T spectrum than those in the nonresonant SM backgrounds.
(iii) Cut 3: The distance between two photons lies in $1.8 < \Delta R_{\gamma_1,\gamma_2} < 3.5$; the distance between the diphoton system and the extra light jet lies in $\Delta R_{\gamma\gamma,j} < 1.8$.
(iv) Cut 4: The invariant mass of the diphoton system, $M_{\gamma\gamma}$, is peaked in both the signals and resonant backgrounds; thus, we require $M_{\gamma\gamma}$ to be in the range $|M_{\gamma\gamma} - m_h| < 2$ GeV.
(v) Cut 5: The transverse mass $M_T(\ell)$ and $M_T(b\ell)$ cuts are $M_T(\ell) > 30$ GeV and 100 GeV $< M_T(b\ell) <$ 180 GeV.
(vi) Cut 6: The invariant mass $M_{\gamma\gamma j}$ cut is 160 GeV $< M_{\gamma\gamma j} <$ 190 GeV.

For the FCC-hh analysis at 100 TeV, we use the same selection cuts for the signal and SM backgrounds because the distributions are very similar to the case of HE-LHC presented in Fig. 3. In fact, the difference between the HE-LHC and FCC-hh mainly comes from the different detector configurations. The effects of the suitable cuts on the signal and SM background processes are illustrated in Table II and Table III at the HE-LHC and FCC-hh, respectively. Due to the different b-tagging rates for u and c quarks, the signal efficiencies of the two top (anti)quark decays differ after applying requirements on the b-tagged jet multiplicity. Thus, we give the events separately for $q = u$, c. One can see that, at the end of the cut flow, the largest SM background is the $pp \to t\bar{t}h$ process, which is about 0.001 fb and 0.02 fb at the HE-LHC and FCC-hh, respectively. Besides, the $tj\gamma\gamma$ process can also generate significant contributions to the SM background due to the large production cross section. Finally, notice that, after the final cuts, the dominant signal contribution comes from the FCNC top (anti)quark decay process, so that one can safely ignore the contribution from the top-Higgs boson associated production channels.

B. Sensitivities at the HE-LHC and FCC-hh

To estimate the exclusion significance, $Z_{\rm excl}$, we use the following expression [75–77]:

$$Z_{\rm excl} = \sqrt{2\left[s - b\ln\left(\frac{b+s+x}{2b}\right) - \frac{1}{\delta^2}\ln\left(\frac{b-s+x}{2b}\right)\right] - (b+s-x)\left(1+\frac{1}{\delta^2 b}\right)}, \tag{7}$$

TABLE II. The cut flow of the cross sections (in ab) for the signals and SM backgrounds at the HE-LHC where the anomalous coupling parameters are taken as $\kappa_{tuh} = 0.04$ or $\kappa_{tch} = 0.04$ in the signal, while fixing the other to zero.

	Signal		Backgrounds					
Cuts	$t\bar{t} \to thu(thc)$	$thu(thc)$	$t\bar{t}h$	thj	$W^{\pm}jjh$	$t\bar{t}\gamma\gamma$	$tj\gamma\gamma$	$\gamma\gamma W^{\pm}jj$
Basic cuts	366 (358)	114 (37)	269	35	20	4064	4880	5985
Cut 1	277 (268)	96 (29)	119	25	16	1819	3660	4988
Cut 2	164 (157)	68 (19)	68	15	8	348	610	855
Cut 3	40 (38)	3.6 (1.3)	10	1.3	0.7	56	74	109
Cut 4	19 (18)	1.7 (0.6)	5	0.6	0.3	1.4	2.1	2.6
Cut 5	13 (13)	1.3 (0.4)	2.2	0.4	0.1	0.6	1.2	0.3
Cut 6	8.9 (7.7)	0.6 (0.2)	0.95	0.16	0.04	0.18	0.42	0.19

TABLE III. The cut flow of the cross sections (in ab) for the signals and SM backgrounds at the FCC-hh, where the anomalous coupling parameters are taken as $\kappa_{tuh} = 0.04$ or $\kappa_{tch} = 0.04$ in the signal, while fixing the other to zero.

	Signal		Backgrounds					
Cuts	$t\bar{t} \to thu(thc)$	$thu(thc)$	$t\bar{t}h$	thj	$W^{\pm}jjh$	$t\bar{t}\gamma\gamma$	$tj\gamma\gamma$	$\gamma\gamma W^{\pm}jj$
Basic cuts	4053 (4364)	1187 (538)	7575	592	324	73800	63000	55158
Cut 1	3262 (2876)	899 (379)	2461	376	252	22140	40320	42795
Cut 2	1879 (1686)	612 (257)	1285	215	144	5535	8820	20446
Cut 3	440 (367)	28 (14)	161	15	10	775	932	2330
Cut 4	396 (327)	25 (12)	142	14	9	16	22	45
Cut 5	282 (221)	18 (9)	59	9	2.6	6.3	13	9
Cut 6	222 (173)	7 (4)	21.6	3	1	1.6	4.2	3.6

with $x = \sqrt{(s+b)^2 - 4\delta^2 s b^2/(1+\delta^2 b)}$. Here, the values of s and b were obtained by multiplying the total signal and SM background cross sections, respectively, by the integrated luminosity. Furthermore, δ is the percentage systematic error on the SM background estimate. In the limit of $\delta \to 0$, this expression can be simplified as

$$Z_{\text{excl}} = \sqrt{2[s - b\ln(1+s/b)]}. \tag{8}$$

In this work, we choose two cases: no systematics ($\delta = 0$) and a systematic uncertainty of $\delta = 10\%$ for both the HE-LHC and FCC-hh. We define the regions with $Z_{\text{excl}} \leq 1.645$ as those that can be excluded at 95% C.L. ($p = 0.05$). The limits on the FCNC coupling parameter κ_{tqh} can be directly translated in terms of constraints on $\text{BR}(t \to qh)$ by using Eq. (2).

In Figs. 4–5, we plot the exclusion limits at 95% C.L. in the plane of the integrated luminosity and the $\text{BR}(t \to qh)$'s at the HE-LHC and FCC-hh with the aforementioned two systematic error cases of $\delta = 0$ and $\delta = 10\%$. One can see that our signals are rather robust against the systematic uncertainties on the background determination, though they differ between the HE-LHC (where limits change within a factor of ≈1.1) and FCC-hh (where limits change within a factor of ≈3.1) due to the relatively different number of SM background events. The values for 95% C.L. upper limits are summarized in Table IV. With a realistic 10% systematic error, the sensitivities are slightly weaker than those without any systematic error, being of the order of 10^{-5} at the 95% C.L. both at the HE-LHC and FCC-hh. For comparison, the recent 95% upper limits on $\text{BR}(t \to qh)$ obtained at the HL-LHC with an integrated luminosity of 3 ab^{-1} by the ATLAS Collaboration [45] are also presented, which are obtained via the decay mode $t \to qh(\to b\bar{b})$. Besides, the upgraded ATLAS experiment has also estimated top-Higgs boson FCNC couplings via the decays $t \to ch(\to \gamma\gamma)$ at the HL-LHC and obtained an expected upper limit of $\text{BR}(t \to ch) < 1.5 \times 10^{-4}$ at 95% C.L. [46]. Altogether, the sensitivity to the BR of the $t \to qh$ are 2 orders of magnitude

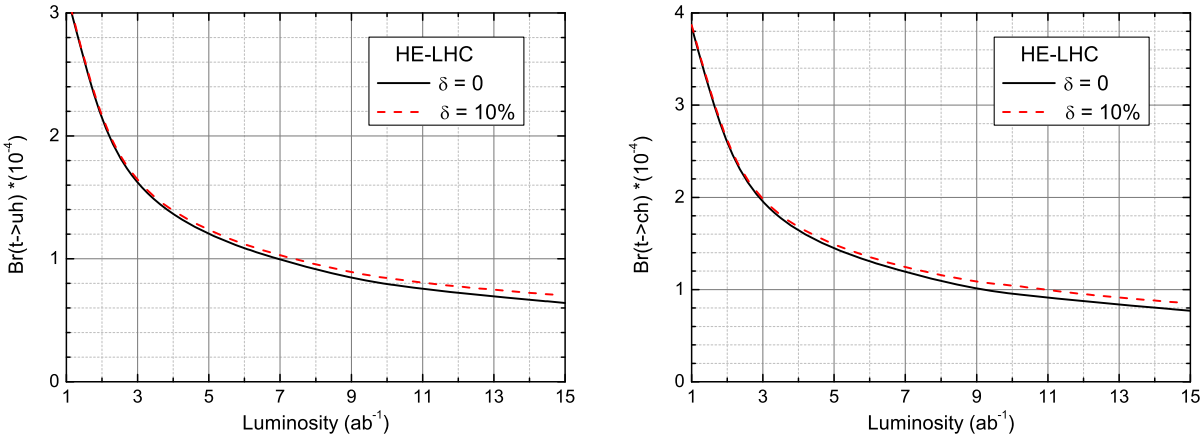

FIG. 4. The exclusion limits at 95% C.L. on $\text{BR}(t \to uh)$ (left) and $\text{BR}(t \to ch)$ (right) at the HE-LHC with two systematic error cases: $\delta = 0$ and $\delta = 10\%$.

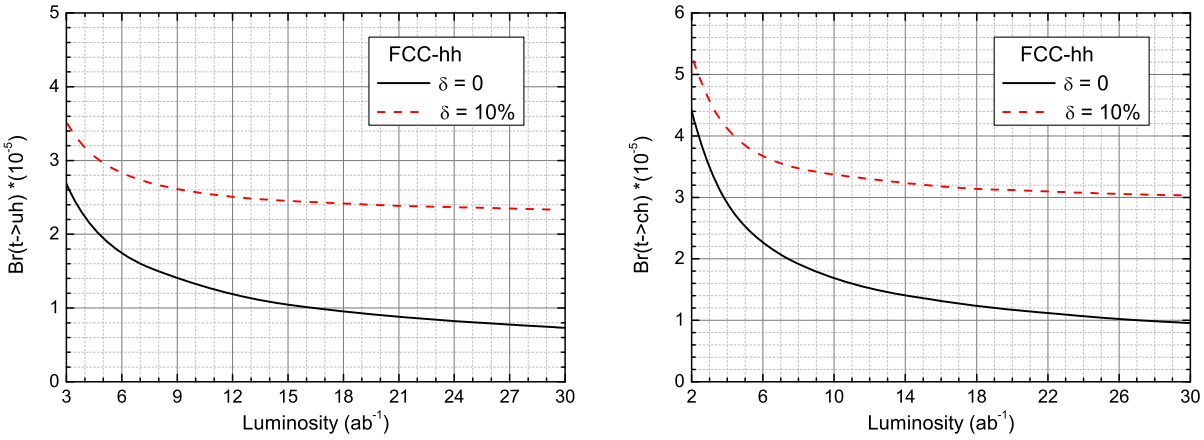

FIG. 5. Same as Fig. 4 but for the FCC-hh.

TABLE IV. The upper limits on BR($t \to qh$) at 95% C.L. obtained at the HE-LHC and FCC-hh. We consider systematic errors of 0% and 10% on the SM background events only. The 95% C.L. upper limits obtained at the HL-LHC at 3 ab^{-1} by the ATLAS Collaboration also have been shown for comparisons.

	HE-LHC, 15 ab^{-1}		FCC-hh, 30 ab^{-1}		
Branching fraction	$\delta = 0$	$\delta = 10\%$	$\delta = 0$	$\delta = 10\%$	HL-LHC, 3 ab^{-1}
BR($t \to uh$)	6.4×10^{-5}	7.0×10^{-5}	7.3×10^{-6}	2.3×10^{-5}	2.4×10^{-4}, $h \to b\bar{b}$ [45]
BR($t \to ch$)	7.7×10^{-5}	8.5×10^{-5}	9.6×10^{-6}	3.0×10^{-5}	1.5×10^{-4}, $h \to \gamma\gamma$ [46]

better than the most recent direct limits reported by the ATLAS Collaboration at the 13 TeV LHC.

Before closing, let us also review competing limits from other authors. Very recently, the author of Ref. [78] has studied the top-Higgs boson FCNC couplings in the triple-top signal at the HE-LHC and FCC-hh. The 95% C.L. upper limits on BR($t \to uh$) [and BR($t \to ch$)] were found, respectively, as $7.01 \times 10^{-4}(3.66 \times 10^{-4})$ at the HE-LHC with 15 ab^{-1} and as $2.49 \times 10^{-5}(5.85 \times 10^{-5})$ at the FCC-hh with 10 ab^{-1}. Furthermore, in the context of the 2-Higgs boson doublet model (2HDM), the authors of Ref. [79] have recently investigated the prospect for $t \to ch$ decay in top quark pair production via the $h \to WW^* \to \ell^+\ell^- + \not{E}_T^{\rm miss}$ channel. For the HE-LHC and FCC-hh, the 95% C.L. upper limits on BR($t \to ch$) was found to be at the order of 10^{-4} with an integrated luminosity of 3 ab^{-1}, and such limits would be increased by an higher integrated luminosity. Finally, at the FCC-hh with an integrated luminosity of 10 ab^{-1}, Ref. [80] has investigated the $t \to ch$ decay, and the its BR can be constrained to $\mathcal{O}(10^{-5})$ either with or without considering c-jet tagging.

IV. SUMMARY

In this work, we have analyzed the process $pp \to thj$ at the HE-LHC and FCC-hh by considering thq FCNC couplings. We have performed a full Monte Carlo simulation for the signals obtained from three different subprocesses via the top leptonic decay mode and $h \to \gamma\gamma$ against all relevant SM backgrounds. After a dedicated cut based selection, we have found that top pair production followed by one FCNC top decay is significantly more abundant than FCNC single top-Higgs boson associated production in presence of a jet. The obtained exclusion limits on the tqh coupling strengths and the ensuing BRs have been summarized and compared in detail to results in literature, namely, the most recent LHC experimental limits and the (projected) HL-LHC ones as well. Our results show that 95% C.L. limits on the BR($t \to qh$), with $q = u(c)$, have been found to be $6.4(7.7) \times 10^{-5}$ at the HE-LHC with an integrated luminosity of 15 ab^{-1} and $7.3\,(9.6) \times 10^{-6}$ at the FCC-hh with an integrated luminosity of 30 ab^{-1}, in the case the SM background is known with negligible uncertainty. When a more realistic 10% systematic uncertainty is considered, the sensitivity decreases to $7.0(8.5) \times 10^{-5}$ at the HE-LHC and $2.3(3.0) \times 10^{-5}$ at the FCC-hh. Remarkably, then, the performance of the two machines is found roughly comparable in this case, i.e., within a factor of $\approx$3. Altogether, these limits are nearly 2 orders of magnitude better than the current experimental results obtained from LHC runs at 13 TeV and 1 order of magnitude better than the existing projections for the HL-LHC at 14 TeV. Therefore, the numerical results presented here for the future HE-LHC and FCC-hh represent good reasons for pursuing further the study of their potential in extracting FCNC effects from NP manifesting themselves in top-Higgs boson interactions.

ACKNOWLEDGMENTS

The work of Y.-B.L is supported by the Foundation of the Henan Educational Committee (Grant No. 2015GGJS-059) and the Foundation of the Henan Institute of Science and Technology (Grant No. 2016ZD01). S. M. is supported in part by the NExT Institute and the STFC CG Grant No. ST/L000296/1.

[1] G. Aad *et al.* (ATLAS Collaboration), Phys. Lett. B **716**, 1 (2012).
[2] V. Khachatryan *et al.* (CMS Collaboration), Phys. Lett. B **716**, 30 (2012).
[3] S. L. Glashow, J. Iliopoulos, and L. Maiani, Phys. Rev. D **2**, 1285 (1970).
[4] B. Mele, S. Petrarca, and A. Soddu, Phys. Lett. B **435**, 401 (1998).
[5] J. A. Aguilar-Saavedra, Acta Phys. Pol. B **35**, 2695 (2004).
[6] J. A. Aguilar-Saavedra, Nucl. Phys. **B821**, 215 (2009).
[7] J. L. Diaz-Cruz, H. J. He, and C. P. Yuan, Phys. Lett. B **530**, 179 (2002).

[8] J. Cao, C. Han, L. Wu, J. M. Yang, and M. Zhang, Eur. Phys. J. C **74**, 3058 (2014).
[9] T. J. Gao, T. F. Feng, F. Sun, H. B. Zhang, and S. M. Zhao, Chin. Phys. C **39**, 073101 (2015).
[10] H. J. He and C. P. Yuan, Phys. Rev. Lett. **83**, 28 (1999).
[11] H. J. He, S. Kanemura, and C. P. Yuan, Phys. Rev. Lett. **89**, 101803 (2002).
[12] C. Kao, H. Y. Cheng, W. S. Hou, and J. Sayre, Phys. Lett. B **716**, 225 (2012).
[13] K. F. Chen, W. S. Hou, C. Kao, and M. Kohda, Phys. Lett. B **725**, 378 (2013).
[14] T. Han and R. Ruiz, Phys. Rev. D **89**, 074045 (2014).
[15] G. Abbas, A. Celis, X. Q. Li, J. Lu, and A. Pich, J. High Energy Phys. 06 (2015) 005.
[16] F. J. Botella, G. C. Branco, M. Nebot, and M. N. Rebelo, Eur. Phys. J. C **76**, 161 (2016).
[17] M. A. Arroyo-Ureña, J. L. Diaz-Cruz, E. Díaz, and J. A. Orduz-Ducuara, Chin. Phys. C **40**, 123103 (2016).
[18] B. Yang, N. Liu, and J. Han, Phys. Rev. D **89**, 034020 (2014).
[19] M. Badziak and K. Harigaya, Phys. Rev. Lett. **120**, 211803 (2018).
[20] V. Khachatryan *et al.* (CMS Collaboration), J. High Energy Phys. 02 (2017) 079.
[21] G. Aad *et al.* (ATLAS Collaboration), J. High Energy Phys. 12 (2015) 061.
[22] M. Aaboud *et al.* (ATLAS Collaboration), J. High Energy Phys. 10 (2017) 129.
[23] M. Aaboud *et al.* (ATLAS Collaboration), Phys. Rev. D **98**, 032002 (2018).
[24] M. Aaboud *et al.* (ATLAS Collaboration), J. High Energy Phys. 05 (2019) 123.
[25] A. M. Sirunyan *et al.* (CMS Collaboration), J. High Energy Phys. 06 (2018) 102.
[26] J. I. Aranda, A. Cordero-Cid, F. Ramirez-Zavaleta, J. J. Toscano, and E. S. Tututi, Phys. Rev. D **81**, 077701 (2010).
[27] F. Larios, R. Martinez, and M. A. Perez, Phys. Rev. D **72**, 057504 (2005).
[28] T. M. P. Tait and C.-P. Yuan, Phys. Rev. D **63**, 014018 (2000).
[29] J. A. Aguilar-Saavedra and G. C. Branco, Phys. Lett. B **495**, 347 (2000).
[30] H. J. He, T. M. P. Tait, and C. P. Yuan, Phys. Rev. D **62**, 011702 (2000).
[31] Q. H. Cao, J. Wudka, and C.-P. Yuan, Phys. Lett. B **658**, 50 (2007).
[32] T. Han, Int. J. Mod. Phys. A **23**, 4107 (2008).
[33] C. Zhang and S. Willenbrock, Phys. Rev. D **83**, 034006 (2011).
[34] E. L. Berger, Q. H. Cao, C. R. Chen, C. S. Li, and H. Zhang, Phys. Rev. Lett. **106**, 201801 (2011).
[35] A. Kobakhidze, L. Wu, and J. Yue, J. High Energy Phys. 10 (2014) 100.
[36] D. Atwood, S. K. Gupta, and A. Soni, J. High Energy Phys. 10 (2014) 057.
[37] X. Chen and L. Xia, Phys. Rev. D **93**, 113010 (2016).
[38] S. Khatibi and M. Mohammadi Najafabadi, Phys. Rev. D **89**, 054011 (2014).
[39] Y. Wang, F. P. Huang, C. S. Li, B. H. Li, D. Y. Shao, and J. Wang, Phys. Rev. D **86**, 094014 (2012).
[40] C. Degrande, F. Maltoni, J. Wang, and C. Zhang, Phys. Rev. D **91**, 034024 (2015).
[41] N. Craig, J. A. Evans, R. Gray, M. Park, S. Somalwar, S. Thomas, and M. Walker, Phys. Rev. D **86**, 075002 (2012).
[42] L. Shi and C. Zhang, Chin. Phys. C **43**, 113104 (2019).
[43] Y. B. Liu and Z. J. Xiao, Phys. Rev. D **94**, 054018 (2016).
[44] H. Sun and X. Wang, Eur. Phys. J. C **78**, 281 (2018).
[45] ATLAS Collaboration, CERN Report No. ATL-PHYS-PUB-2016-019, 2016.
[46] ATLAS Collaboration, ATL-PHYS-PUB-2013-012, 2013.
[47] P. Mandrik (FCC Study Group), J. Phys. Conf. Ser. **1390**, 012044 (2019).
[48] M. Benedikt and F. Zimmermann, Nucl. Instrum. Methods Phys. Res., Sect. A **907**, 200 (2018).
[49] N. Arkani-Hamed, T. Han, M. L. Mangano, and L.-T. Wang, Phys. Rep. **652**, 1 (2016).
[50] X. Cid Vidal *et al.*, (Working Group 3), arXiv:1812.07831.
[51] M. Cepeda *et al.*, (HL/HE WG2 Group), arXiv:1902.00134.
[52] P. Azzi *et al.*, (HL-LHC Collaboration and HE-LHC Working Group), arXiv:1902.04070.
[53] ATLAS and CMS Collaborations, arXiv:1902.10229.
[54] L. Wu, J. High Energy Phys. 02 (2015) 061.
[55] Y. B. Liu and Z. J. Xiao, Phys. Lett. B **763**, 458 (2016).
[56] C. S. Li, R. J. Oakes, and T. C. Yuan, Phys. Rev. D **43**, 3759 (1991).
[57] A. Greljo, J. F. Kamenik, and J. Kopp, J. High Energy Phys. 07 (2014) 046.
[58] Y. B. Liu and S. Moretti, Chin. Phys. C **43**, 013102 (2019).
[59] J. J. Zhang, C. S. Li, J. Gao, H. Zhang, Z. Li, C.-P. Yuan, and T. C. Yuan, Phys. Rev. Lett. **102**, 072001 (2009).
[60] J. Drobnak, S. Fajfer, and J. F. Kamenik, Phys. Rev. Lett. **104**, 252001 (2010).
[61] C. Zhang and F. Maltoni, Phys. Rev. D **88**, 054005 (2013).
[62] A. Alloul, N. D. Christensen, C. Degrande, C. Duhr, and B. Fuks, Comput. Phys. Commun. **185**, 2250 (2014).
[63] J. Alwall, R. Frederix, S. Frixione, V. Hirschi, F. Maltoni, O. Mattelaer, H.-S. Shao, T. Stelzer, P. Torrielli, and M. Zaro, J. High Energy Phys. 07 (**2014**) 079.
[64] R. D. Ball *et al.* (NNPDF Collaboration), J. High Energy Phys. 04 (2015) 040.
[65] M. Tanabashi *et al.* (Particle Data Group), Phys. Rev. D **98**, 030001 (2018).
[66] J. Alwall *et al.*, Eur. Phys. J. C **53**, 473 (2008).
[67] J. Alwall, S. de Visscher, and F. Maltoni, J. High Energy Phys. 02 (2009) 017.
[68] T. Sjöstrand, S. Ask, and J. R. Christiansen, R. Corke, N. Desai, P. Ilten, S. Mrenna, S. Prestel, C. O. Rasmussen, and P. Z. Skands, Comput. Phys. Commun. **191**, 159 (2015).
[69] J. de Favereau, C. Delaere, P. Demin, A. Giammanco, V. Lemaître, A. Mertens, and M. Selvaggi (DELPHES 3 Collaboration), J. High Energy Phys. 02 (2014) 057.
[70] E. Conte, B. Fuks, and G. Serret, Comput. Phys. Commun. **184**, 222 (2013).
[71] M. Cacciari, G. P. Salam, and G. Soyez, Eur. Phys. J. C **72**, 1896 (2012).
[72] M. L. Mangano *et al.*, CERN Yellow Report (CERN, Geneva, 2017), Vol. 3, pp. 1–254.

[73] M. Cepeda *et al.*, CERN Yellow Report Monographs (CERN, Geneva, 2019), Vol. 7, p. 221.
[74] Y. Zhang, W. G. Ma, R. Y. Zhang, C. Chen, and L. Guo, Phys. Lett. B **738**, 1 (2014).
[75] G. Cowan, K. Cranmer, E. Gross, and O. Vitells, Eur. Phys. J. C **71**, 1554 (2011); **73**, 2501(E) (2013).
[76] N. Kumar and S. P. Martin, Phys. Rev. D **92**, 115018 (2015).
[77] F. Kling, H. Li, A. Pyarelal, H. Song, and S. Su, J. High Energy Phys. 06 (2019) 031.
[78] H. Khanpour, arXiv:1909.03998.
[79] R. Jain and C. Kao, Phys. Rev. D **99**, 055036 (2019).
[80] A. Papaefstathiou and G. Tetlalmatzi-Xolocotzi, Eur. Phys. J. C **78**, 214 (2018).